# MEANS FOR MEASURING THE ELECTRIC AND MAGNETIC QUANTITIES

## HARDWARE-SOFTWARE EMBEDDED SYSTEM OF SIGNAL FREQUENCY SELECTION ON GYRATOR

***Grygorii Barylo, Dr.Sc., Ass. Prof., Igor Helzhynskyy, Ph.D., Ass. Prof., Tetyana Marusenkova, Ph.D., Ass. Prof., Yurii Kryvenchuk, Ph.D., Ass. Prof., Mykola Khilchuk, Ph.D. student***
*Lviv Polytechnic National University, Ukraine; e-mail:yurkokryvenchuk@gmail.com*
***Roman Holyaka, Dr. Sc., Prof., Oksana Boyko, Dr.Sc., Ass. Prof.***
*Danylo Halytsky Lviv National Medical University, Ukraine*

**Abstract.** The work is devoted to the problem of frequency-selective signal conversion in microelectronic sensor devices. It has been shown that the signal path of such devices, in particular, sensor nodes in the concept of the Internet of Things, must meet the requirements of embedded systems using a mixed analog-digital front end. The analysis of the signal transformation of photovoltaic sensors, in particular the problem of a significant parasitic influence of extraneous non-informative optical radiation and electromagnetic interference, has been carried out. SPICE models of photovoltaic sensor signal circuits providing frequency selection on bandwidth filters have been synthesized. The main approaches of hardware-software implementation of the built-in system of frequency selection with the mixed-signal transformation are considered. The signal path of the embedded system includes a gyrator, a software-controlled amplifier, a synchronous demodulator, an analog-to-digital converter, and a digital filter. The implementation is carried out on the platform of the programmable system on a PSoC chip. The integrated circuits of the PSoC 5 LP Family Cypress Semiconductor Corporation are used with a wide range of programmable analog front-end nodes, in particular operating amplifiers, comparators, units on switching capacitors, reference voltage sources on the principle of the forbidden zone, analog multiplexers, signal synthesizers, etc. The efficiency of the mixed analog and digital signal conversion is shown.

**Key words:** Signal Processing, Frequency Selection, Programmable System on Chip, Sensor Nodes Front-End, Optical Sensors in IoT concept.

### 1. Introduction

Electronic means of information and computer technologies are currently one of the most dominant engines of technical development in modern society. In addition to the traditionally electronic branches of technology – radio, telecommunications, information and measurement, computer technology, etc., electronics and devices based on them have become important tools for the development of industry, biology, medicine, ecology, etc. The implementation of modern electronic devices in these areas is based on the concept of embedded systems

Sensors, actuators, and signal transducers are the basis of electronics interaction with the physical world and have been named Analog Front-end (AFE) [2]. The combination of analog front-end nodes and digital signal processing is demonstrated in publications on the implementation of Mixed-Signal Embedded System [3] and Heterogeneous Embedded Systems [4] of signal transformation. The urgency of the problem of developing and using such embedded systems is due to the modern concept of the Internet of Things IoT [5].

Examples of analog and mixed IoT front-end are built-in capacitive accelerometer systems (Capacitive MEMS Accelerometer Analog Front-End for Ultra-Low-Power IoT Applications) [6] and underwater sensor networks (Analog-to-Digital Acquisition Channel for an IoT Water Management Sensor Node) [7]. Emphasis is placed on the relevance of the low-power low-noise inductorless front-end for IoT applications [8].

Following modern trends in the development of embedded systems of mixed-signal conversion, this article deals with the approaches of hardware-software realization of the signal tract of sensor devices with a high level of frequency selection. The signal path is implemented on the platform of the programmable system on the PSoC (Programmable System on Chip) [9] with the API control. The efficiency of the combination of analog and digital signal conversion is shown. The basis of the analog path is a gyrator [10], non-inductive frequency-selective trans-impedance (TIA – Trans-Impedance Amplifier) conversion [11], and a digital path – a bandpass filter of FIR (Finite Impulse Response) type. Also, the signal path includes a software-controlled amplifier PGA (Programmable Gain Amplifier), a synchronous demodulator based on a multifunction mixer MIX, a delta-sigma Analog-to-Digital Converter, and a serial UART interface that provides its high versatility in various embedded front-end systems of microelectronic IoT sensors.

The object of research of this work will be demonstrated on the example of the construction of functionally integrated photovoltaic sensor nodes of the info-communication system of the WSN (Wireless Sensor Network) in the concept of Data Fusion. Other

related terms of this concept are Sensor Data Fusion, or in a shorter form, Sensor Fusion [12]. Such sensor devices and info-communication systems based on them are defined by the concepts of Smart Sensors [13] and Lab-on-Chip [14] with telecommunications per wireless optical communication technologies: OWC – Optical Wireless Communications, FSO – Free Space Optical communication, VLC – Visible Light Communication [15].

## 2. Formulation of the problem

The informative value of photovoltaic sensors is the color (optical absorption spectrum) of the active medium (analyte, in particular, in the form of a thin-film chemically active structure) that interacts with the investigated components (impurities, contaminants, etc.) in the atmosphere, solutions or surfaces. For this purpose, the transmitter generates sequences of pulses the luminous flux of different spectrums. The receiver receives and converts these luminous fluxes into control signals, supplies energy and spectral components of the optoelectronic sensor signal.

The main problem of photovoltaic sensors is the significant parasitic effect of extraneous (non-informative) optical radiation and electromagnetic interference. Thus, the intensity of radiation of extraneous light sources (sun, light bulbs, etc.) in hundreds or even thousands, times exceeds the useful component of the optical signal change from the active medium, the spectral characteristic of which carries information about the investigated chemical or biochemical substance. A typical solution to the above problem by dimming extraneous light sources contradicts the requirement for the openness of the active medium, which involves the effective interaction of this medium with its surroundings. It is inefficient to solve the problem of optical filters. First, the efficiency of spectral selection of optical filters is not high, and secondly, the use of such filters limits the informativeness of the useful signal. The parasitic effect of electromagnetic interference is primarily due to the radiation of the power grid with a frequency of 50 Hz. The intensity of such radiation is typically significant, and the shielding of the optoelectronic pair of the sensor device contradicts the same requirement for its openness.

The parasitic influence of external optical radiation and electromagnetic interference is particularly evident in optoelectronic sensor devices on photodiode transducers. The informative signal of such converters is a photocurrent, that is, the latter implements a measuring circuit with the current output.

The difference between signal converters with current and voltage output will be considered on the example of bandpass filters. For this purpose, we synthesize SPICE models of elementary signal circuits of frequency selection on passive bandpass filters (Fig. 1, left), where C1, R1, and C2, R2 are upper-frequency filters, and C3, R4, and C4, R5 is lower-frequency filters. The signal model of the primary converter of the potentiometric type is represented by the voltage source $V_1$. To implement the model of the primary converter with current output, the functional component of the controllable current source $G_1$ (I of V dependent source), the initial circle of which is shunted by the resistor $R_G$, is used. This resistor (in the given example – $R_G$ = 1E5 Ohm) in the current output converter model represents its output resistance (for the ideal current overpower ($R_G \to \infty$)

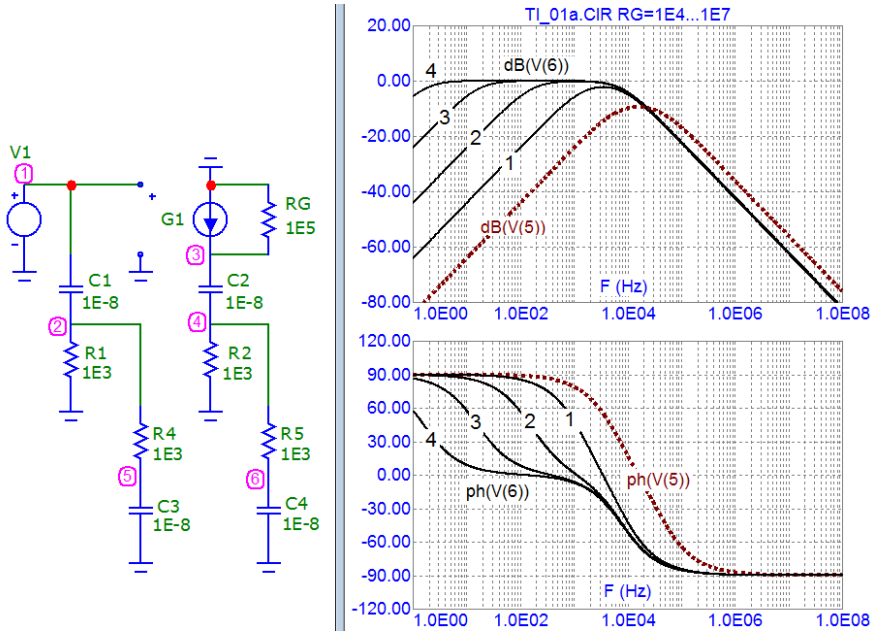


*Fig. 1. Comparison of frequency response (top) and phase response (bottom) circuits of frequency-selective converters (left) with potentiometric (V (5)) and current (V (6)) output at: $R_G$ = 1E4 (1), 1E5 (2), 1E6 (3), 1E7 (4)*

To compare the filtering process of the signals of both types of converters in the normalized form and taking into account the filter input impedance (in particular, taking into account the resistance of their resistors R1 = R2 = R3 = R4 = 1E3 Ohm), the voltage conversion coefficient – the current of the $G_1$ transducer is $K_G$ = 1E3 A/V. The output signal of the bandpass filter of the potentiometric converter is represented by the voltage V (5), and the converter with current output is represented by the voltage V (6).

The results of comparative model studies of frequency response and phase-response characteristics of these filters are presented (Fig. 1, to the right) by transmission coefficients dB(V(5)), dB(V(6)) in dB, and phase delays ph(V(5)), ph(V(6)) in degrees. Investigations were conducted on the set of values of the output resistance of the converter with current output $R_G$ = 1E4 (1), 1E5 (2), 1E6 (3), 1E7 (4)).

The solution to this problem is based on the use in the signal circuit of measuring converters with current output the specialized filters on gyrators – functional circuit nodes of reactive impedance conversion, synthesizing reactive load of inductive type using only capacitive components. A modern representative of specialized signal transducers of optical sensors based on gyrators is the integrated circuit E909.07 (Transimpedance amplifier with high sensitivity) [16].

However, the use of such specialized integrated circuits in microelectronic sensors, in particular the IoT concept, increases their size and energy consumption and is undesirable. Thus, the solution to the problem of further development of photovoltaic microelectronic sensors involves the development of integrated signal transformation systems with single-chip integration of all components of their front end.

## 3. The goal of the work

The purpose of the work is the structural synthesis, circuit implementation, and research of the parameters of the hardware-software embedded system of photovoltaic microelectronic sensors, ensuring efficient frequency selection of the signal using single-chip systems on the crystal.

## 4. Block diagram and operation of the signal path

Following the above requirements, the signal path of the embedded system of photovoltaic microelectronic sensors is implemented on the platform of the embedded programmable system on the PSoC 5 LP with a wide range of software-controlled AFE nodes, comparators, blocks on switching capacitors, reference voltage sources on the principle of the forbidden zone, analog multiplexers, signal synthesizers, etc.

The main components of the signal path (Fig. 2) of the developed embedded PSoC system are the $Z_X$ that is the primary converter of the sensor device, in particular, the photodiode; GAF (analog front-end based on the gyrator scheme); PGA amplifier with programmable gain $K_V$; SD that is the detector based on synchronous demodulator with control of synchronizing pulses CP; Sigma-Delta ADC; DMA; DF (the digital bandpass filter). The output digital signal $D_{OUT}$ is transmitted using a wired or wireless interface. The control modes of the signal path nodes are controlled by the API commands.

The scheme of the gyrator is implemented on the operational amplifier operating in the mode of the voltage follower, and passive components – $R_1$, $R_2$, $C_1$. The capacitor $C_2$ is auxiliary and used only if the selection coefficient is further increased. The functioning of this scheme is described by a system of equations of a functional connection between the vectors of currents I , voltages U , and complex resistances, the indices of the symbols of which are determined by the symbols of the components in Fig 2:

$$\begin{cases} \dot{I}_{IN} = \dot{I}_{R1} + \dot{I}_{R2} \\ \dot{U}_{R2} = \dot{U}_{C1} \\ \dot{U}_Z = \dot{I}_{IN}\dot{Z}_{IN} \\ \dot{U}_Z = \dot{U}_{C1} + \dot{U}_{R1} \end{cases}$$

To approximate the frequency dependency of the input impedance $Z_{IN}$ by replacing current and voltage vectors with their modular values $\dot{U} \Rightarrow U$, $\dot{I} \Rightarrow I$, write down

$$U_{C1} = U_Z - U_{R1}; \qquad I_{C1} = \frac{U_Z}{Z_{C1} + R_1};$$

$$Z_{C1} = \frac{1}{\omega C_1}; \qquad I_{R2} = U_Z \frac{Z_{C1}}{(Z_{C1} + R_1)R_2}.$$

After corresponding transformations of these expressions, we receive

$$Z_{IN} = \frac{(1 + \omega R_1 C_1)R_2}{1 + \omega R_2 C_1}.$$

This calculation does not take into account the phase shift of the vectors of voltage and current. It represents only the first approximation, so it is still possible to identify certain patterns of frequency dependence of the input impedance $Z_{IN}$. In particular, at low frequencies ($\omega \to 0$) the input impedance approaches $Z_{IN} \to R_2$. Instead, at high frequencies ($\omega \to \infty$) takes place $Z_{IN} \to R_1$.

Thus, changing the ratio between the resistors $R_1$ and $R_2$ is possible to synthesize the impedance both capacitive ($R_1 / R_2 < 1$), and inductive ($R_1 / R_2 > 1$) character. In particular, with increasing frequency at $R_1 / R_2 = 10^4$ we obtain the raising an impedance, in dB:

$$K_{ZIN}\,(\text{dB}) = K_{ZIN}\,(\omega \to \infty) / K_{ZIN}\,(\omega \to 0) =$$
$$= 20 \log (10^4) = 80 \text{ dB}.$$

Examples of SPICE model studies of the parameters of the considered gyrator scheme, which confirm the above calculations and give more accurate data taking into account the phase characteristics of the signal path, are shown in Fig. 3. The model of the Primary transducer GPHD is represented by the input voltage source $V_{IN}$, voltage-current converter V-> I, and diode $D_1$, the parameters of which characterize the corresponding characteristics of the photodiode. The voltage repeater is represented by the circuit component $X_1$.

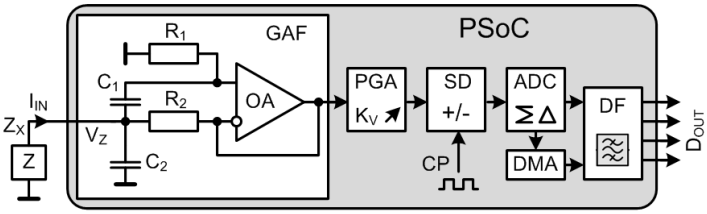


*Fig. 2. Block diagram of the signal path*

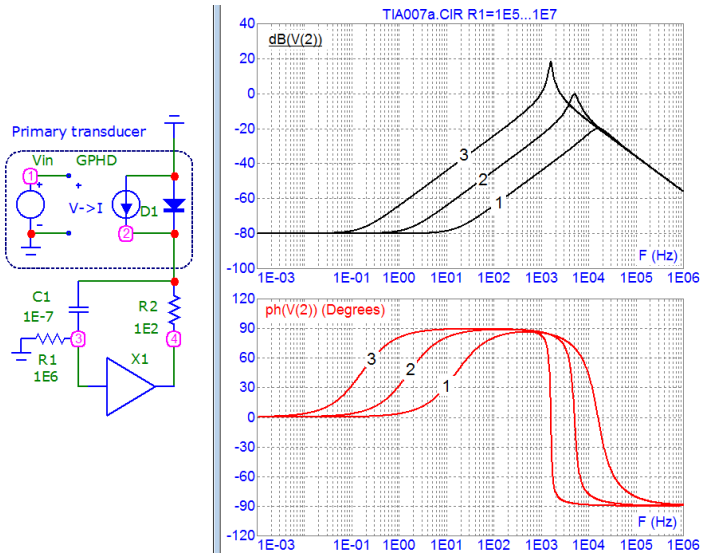


*Fig.3. Frequency response (top) and phase response (bottom) of gyrator circuit at $R_1$ = [1E5 (1), 1E6 (2), 1E7 (3)] Ohm*

The results of model research of frequency response and phase response of the signal circuit are represented (Fig. 3, right) by voltage conversion coefficients dB (V (2)) in dB and phase delays ph (V (2)) in degrees. These coefficients characterize the effect of increasing the impedance of the gyrator in node 2 in the frequency selection of the informative signal. Researches were performed to set the resistance values of the resistor $R_1$ = [1E5 (1), 1E6 (2), 1E7 (3)] Ohm. It can be seen that the considered scheme of the gyrator provides the possibility of high-frequency signal selection in circuits with the current output of the primary converter. Thus, at $R_1$ = 1E6 Ohm the selection coefficient is $K_{ZIN}\approx$ 80 dB, and at $R_1$ = 1E6 Ohm – $K_{ZIN}\approx$ 100 dB. The frequency band of the signal selection is determined by the RC parameters of the gyrator circuit, the parasitic capacitance of the primary converter (in this case – the diode $D_1$ structure of the photodiode), and the frequency response of the operational amplifier in the mode of voltage repeater (in this case – component $X_1$). Further increase of frequency selection is provided by stages of synchronous detection of a signal and its digital filtering.

## 5. Implementation and parameters of hardware-software embedded system

The signal path of the built-in programmable sensor photovoltaic device system is implemented on the components of the PSoC 5 LP (Fig. 4). It includes the considered above gyrator on the operational amplifier Opamp_1, two cascades on programmable amplifiers PGA_1 and PGA_2, a signal generator on a digital-analog converter WaveDAC8_1 (8-bit Waveform Generator), the synchronous detector on the mixer Mixer_1, ADC_DelSig_1 with DMA_1 data recording in RAM, software-controlled digital filter Filter_1, Vref Reference Voltage (Vdda/2) Generator, serial asynchronous interface UART and some other components. These are, in particular, auxiliary nodes of the signal shaper – timer Timer_1, controlling register Control_Rg_1, frequency divider FreqDiv_1, etc.

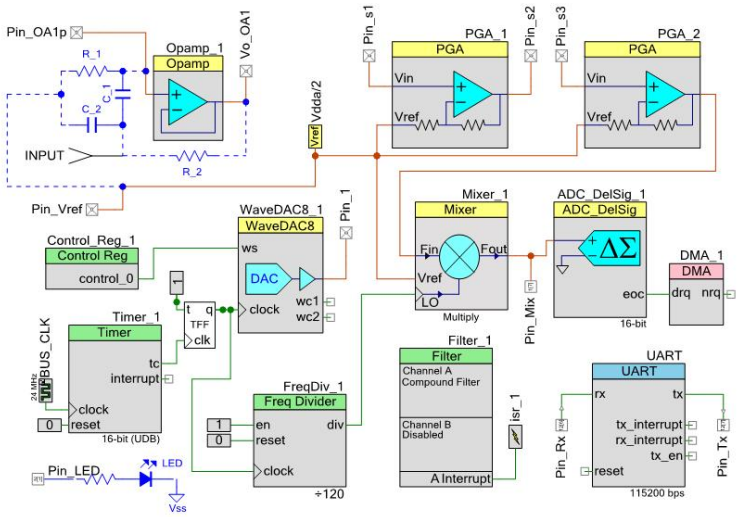


*Fig. 4. The scheme of the signal path on the PSoC components*

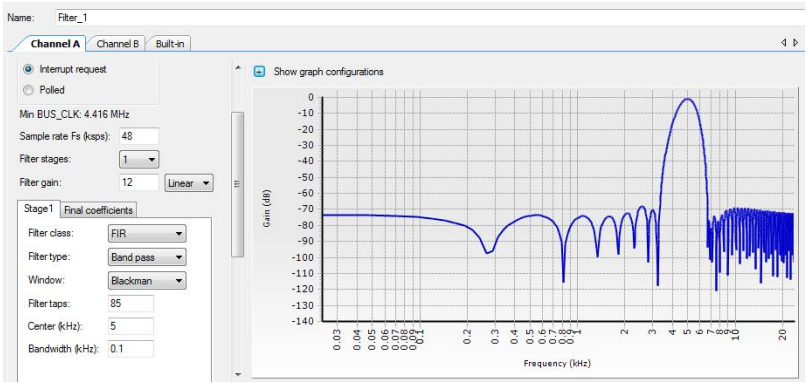


*Fig. 5. Software control window of the digital filter and its frequency response*

Most of the components of the embedded system provide the ability to control the operation modes programmatically. In particular, Fig. 5 shows the software control window of a digital filter, the operating modes and frequency response of which are controlled by parameters such as filter class, filter type, the number of conversion stages Filter stage, Filter gain, the central frequency of the filter band Center (kHz) and bandwidth Bandwidth (kHz). Depending on these parameters and measurement modes, the signal selection factor is within the range of 40 … 80 dB.

The layout of the developed embedded system of signal frequency selection on PSoC and windows of the control of the operating mode software are presented in Fig. 6. The interface of the measurement modes control software provides a possibility of a choice the frequency and the form of the giving signal, gain, filtering parameters, interface parameters, etc. The measurement results are visualized in two graphical windows Data Graph 1 and Data Graph 2.

The main parameters of the developed embedded frequency selection system are the supply voltage 5 V; the supply current – no more than 20 mA; the frequency band – from 1 Hz to 100 kHz; the shape of the master signal – rectangular, sun-shaped, triangular; the signal amplification factor – from 1 to 10000; the useful signal selection factor – up to 140 dB.

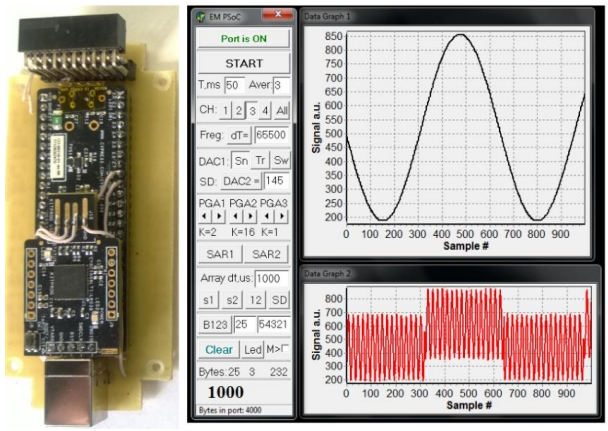


*Fig. 6. The layout of the embedded system on PSoC and software windows*

## 6. Conclusions

The problems of signal conversion of photo-voltaic sensors are disclosed, in particular, the significant

influence of parasitic influence of extraneous non-informative optical radiation and electromagnetic interference. It is shown that the signal path of sensor devices must meet the requirements of embedded systems using a mixed analog-digital front-end as also to be based on gyrators – functional circuit nodes of reactive impedance conversion, synthesizing reactive load of inductive type using exceptionally the capacitive components.

The synthesis of SPICE models and the analysis of the parameters of the signal circuits of photovoltaic sensors providing the frequency selection on bandpass filters are performed. The signal path is implemented on a programmable system platform on a PSoC crystal 5 LP with a wide range of software-controlled analog front-end.

In addition to photovoltaic sensors, the presented system has been tested in several of our developments of information-measuring devices, in particular, in devices of spatial tracking on magnetic coils [17, 18]; impedance measuring transducers [19]; thermal analysis devices [20].

## 7. Conflict of Interest

The authors claim that there are no possible financial or other conflicts over the work.

## References

[1] J. Huang, R. Li, J. An, D. Ntalasha, F. Yang, K. Li, "Energy-Efficient Resource Utilization for Heterogeneous Embedded Computing Systems", IEEE Transactions on Computers, vol. 66, no. 9, pp. 1518 – 1531, 2017.

[2] H. Hu, T. Islam, A. Kostyukova, S. Ha, S. Gupta, "From Battery Enabled to Natural Harvesting: Enzymatic BioFuel Cell Assisted Integrated Analog Front-End in 130nm CMOS for Long-Term Monitoring", IEEE Transactions on Circuits and Systems, vol. 66, no. 2, pp. 534 – 545, 2019.

[3] B. Kim, "Dithering Loopback-Based Prediction Technique for Mixed-Signal Embedded System Specifications", IEEE Transactions on Circuits and Systems II: Express Briefs, vol. 63, no. 2, pp. 121 – 125, 2016.

[4] G. Xie, Y. Chen, Y. Liu, Y. Wei, R. Li, K. Li, "Resource Consumption Cost Minimization of Reliable Parallel Applications on Heterogeneous Embedded Systems", IEEE Transactions on Industrial Informatics, vol. 13, no. 4, pp. 1629 – 1640, 2017.

[5] D. Jo, G. Kim, "ARIoT: scalable augmented reality framework for interacting with Internet of Things appliances everywhere", IEEE Transactions on Consumer Electronics, vol. 62, no. 3, pp. 334 – 340, 2016.

[6] I. Akita, T. Okazawa, Y. Kurui, A. Fujimoto, T. Asano, "A Feedforward Noise Reduction Technique in Capacitive MEMS Accelerometer Analog Front-End for Ultra-Low-Power IoT Applications", IEEE Journal of Solid-State Circuits, vol. 55, no. 6, pp. 1599 – 1609, 2020.

[7] H. Serra, I. Bastos, J. L. A. de Melo, "A 0.9-V Analog-to-Digital Acquisition Channel for an IoT Water Management Sensor Node", IEEE Transactions on Circuits and Systems II: Express Briefs, vol. 66, no. 10, pp. 1678 – 1682, 2019.

[8] Yu. Yang, J. Yang, "Low-power low-noise inductorless front-end for IoT applications", *6th International Symposium on Next Generation Electronics (ISNE)*, 2017.

[9] PSoC® 5LP, CY8C52LP Family Datasheet. Programmable System-on-Chip, 2019. [Online]. Avialable: https://www.cypress.com/file/45916/download.

[10] R. Barazarte, G. Gonzalez, M. Ehsani, "Generalized Gyrator Theory", IEEE Transactions on Power Electronics, vol. 25, no. 7, pp. 1832 – 1837, 2010.

[11] R. Chen, Z. Yang, "CMOS Transimpedance Amplifier for Visible Light Communications", IEEE Transactions on Very Large-Scale Integration Systems, vol. 23, no. 11, pp. 2738 – 2742, 2015.

[12] F. Alam, R. Mehmood, I. Katib, N. Albogami, A. Albeshri, "Data Fusion and IoT for Smart Ubiquitous Environments: A Survey", IEEE Access, vol. 5, pp. 9533 – 9554, 2017.

[13] E. Song, G. FitzPatrick, K. Lee, "Smart Sensors and Standard-Based Interoperability in Smart Grids", IEEE Sensors Journal, vol. 17, no. 23, pp. 7723 – 7730, 2017.

[14] A. Grimmer, W. Haselmayr, R. Wille, "Automated Dimensioning of Networked Labs-on-Chip", IEEE Transactions on Computer-Aided Design of Integrated Circuits and Systems, vol. 38, no. 7, pp. 1216 – 1225, 2019.

[15] W. Xu, J. Wang, H. Shen, H. Zhang, X. You, "Indoor Positioning for Multiphotodiode Device Using Visible-Light Communications", IEEE Photonics Journal, vol. 8, no. 1, 2016.

[16] Transimpedance amplifier with high sensitivity E909.07, ELMOS Semiconductor AG, Data Sheet, 2014. [Online]. Available: m: http://www.elmos.com.

[17] R. Holyaka, T. Marusenkova, D. Fedasyuk, "Signal model for spatial position sensors in magnetic tracking systems", Innovative Technologies and Scientific Solutions for Industries, no. 1, pp. 5–18, 2020.

[18] R. Holyaka, T. Marusenkova, D. Fedasyuk, "Measuring logarithmic signal converter for magnetic tracking systems", Measuring Equipment and Metrology, vol. 81, no. 1, pp. 16–21, 2020.

[19] G. Barylo, R. Holyaka, I.Prudyus, S. Fabirovskyy, "Technique of increasing the impedance measuring transducers accuracy at inharmoniousness signals", Visn. NTUU KPI, Seriia – Radiotehnika Radioaparatobuduvannia, no. 70, pp. 30–36, 2017.

[20] O. Boyko, R. Holyaka, Z. Hotra, A. Fechan, H. Ivanyuk, O. Chaban, T. Zyska, I. Shedreyeva, "Functionally integrated sensors of thermal quantities based on optocoupler", In Photonics Applications in Astronomy, Communications, Industry, and High-Energy Physics Experiments. International Society for Optics and Photonics, vol. 10808F, 2018.